2020

Osseodensification-induced bone healing in mouse calvaria under static condition

BOSTON UNIVERSITY

HENRY M. GOLDMAN SCHOOL OF DENTAL MEDICINE

THESIS/DISSERTATION

OSSEODENSIFICATION-INDUCED BONE HEALING IN MOUSE CALVARIA
UNDER STATIC CONDITION

by

BUSHRA A M A AHMAD

BSc. Kuwait University, 2012
BDM. Kuwait University, 2015

Submitted in partial fulfillment of the requirements for the degree of

Master of Science in Dentistry
In the Department of Periodontology

2020

First Reader_____

Dr. Taisuke Ohira, DDS, Ph.D.

Clinical Assistant Professor of Periodontology

Second Reader_____

Dr. Wayne Gonnerman, Ph.D.

Assistant Professor of Periodontology

Third Reader_____

Dr. Serge Dibart, D.M.D

Chair and Professor of Periodontology

ACKNOWLEDGMENTS

OSSEODENSIFICATION-INDUCED BONE MODIFICATION IN MOUSE CALVARIA: STATIC CONDITION

BUSHRA A M A AHMAD

Boston University, Henry M. Goldman School of Dental Medicine, 2020

Dr. Taisuke Ohira, Clinical Assistant Professor

ABSTRACT

Background:

Recently osseodensification has been introduced as a novel approach to management of the recipient site. The concept had been described in 2013 by Huwais which has revolutionized the way we approach an osteotomy site as we may obtain densification of the bone rather than its complete removal.

Aim:

We hypothesize that proper manipulation of the recipient site will induce cellular activities to accelerate new bone formation. We compared bone formation in a critical defect created by the osseodensification method or regular osteotomy under ex-vivo static calvarial culture.

Materials and Methods:

Under sterile conditions, calvaria from 7-9-day-old neonatal CD-1 mice (n = 15) were dissected and trimmed. Densah™ burs were used to create 2.0 mm diameter defects. Clockwise rotation of the bur produced "Conventional Osteotomy," whereas counter-clockwise rotation created "Osseodensification." Five randomly selected calvaria halves

for control and test groups were used to evaluate morphological changes, at 7, 14, and 28 days utilizing the Image J software. Statistical analyses were performed using SPSS software.

Results:

Defect closure was significantly greater in the osseodensification group compared to the conventional group at post-operative day7 ($p = 0.028$), day 14 ($p = 0.046$) and day 28 ($p=0.015$). The original defects in both groups were not significantly different.

Conclusion:

Results showed that osseodensification lead to faster wound healing. Clinical studies have shown that osseodensification leads to better bone density around implants. These outcomes suggest that the compressed edge of a bone defect can accelerate the healing cascade by increasing cellular activity.

TABLE OF CONTENTS

LIST OF TABLES

LIST OF FIGURES

LIST OF ABBREVIATIONS

RANK…………………………..…… Receptor Activator of Nuclear factor-kappa beta

RANKL………………………..………………………………..RANK ligand

BMP………………………..…….………………. Bone morphogenetic proteins

M-CSF…………………………..…………… Macrophage-Colony Stimulating Factor

SNO…………………………….…………….. Spindle-shaped N-cadherin Osteoblasts

PDL……………………………….…………………………… Periodontal ligament

FGF……………………………….……………………..Fibroblast Growth Factor

OPG……………………………….………………………………… Osteoprotegerin

CHAPTER 1
INTRODUCTION

1.1. Cells associated with bone morphology

The success of periodontal treatment, including dental implants, is highly dependent on the biological basis of bone homeostasis. Several highly differentiated cells participate in bone metabolism, including osteocytes, osteoclasts, and osteoblasts (Raggatt and Partridge, 2010). Their cell-cell interactions including receptor-ligand maintain bone stability and mediate bone remodeling.

1.2. Osteoclast

A prime feature of osteoclast precursors is the expression of RANK (Receptor Activator of Nuclear factor-kappa beta), which is the receptor for the RANK ligand (RANKL), on the surface of the cell (Raggatt and Partridge, 2010). This receptor-ligand interaction (RANK-RANKL) plays a pivotal role in osteoclastogenesis and the development of mature osteoclasts (Khosla, 2001). In addition, osteoblast lineage cells (osteoblasts and osteocytes) express Osteoprotegerin (OPG) as a secreted decoy receptor blocker against RANKL. It binds to pre-osteoclasts via RANK and prohibits differentiation and activation of mature osteoclasts.

1.3 Osteoblast

The osteoblast, a primary cell for bone formation, accounts for 4-6% of total resident cells in the bone (Capulli et al., 2014). Osteoblasts express parathyroid hormone receptors and synthesize collagen and non-collagen proteins to aid in the formation of bone matrix

(Raggatt and Partridge, 2010). Osteoblasts are derived from embryonic pluripotent stem cells that can differentiate into many cell types (Raggatt and Partridge, 2010). Osteoblasts mainly produce Receptor Activator of Nuclear Kappa B ligand (RANKL) and osteoprotegerin (OPG) as a positive and negative regulator of osteoclast differentiation, respectively. Osteoblasts bind to osteoclast precursors via RANKL-RANK interaction to activate osteoclast differentiation (Suda T, Takahashi N, Udagawa N, Jimi E, Gillespie MT, Martin TJ. Modulation of osteoclast differentiation and function by the new members of the tumor necrosis factor receptor and ligand families. Endocr Rev. 1999;20:345–357). Secreted OPG from osteoblasts binds to RANKL as a decoy receptor to prevent osteoclasts differentiation (Simonet WS, Lacey DL, Dunstan CR, et al. Osteoprotegerin: a novel secreted protein involved in the regulation of bone density. Cell. 1997;89:309–319). Runx2 (Runt-related transcription factor 2), a transcription factor, also known as Cbfa1 (core-binding factor subunit alpha-1), is a master regulator for pluripotent stem cells to differentiate into osteoblasts and allow proper bone formation (Byers and Garcia, 2004). Runx2 is the product of one of three mammalian genes that encode proteins homologous to Drosophila Runt. It is necessary for proper embryonic development. It regulates mesenchymal condensation, osteoblast differentiation from mesenchymal stem cells, chondrocyte hypertrophy, and vascular invasion during skeletal development (Komori et al., 1997; Otto et al., 1997). Overexpression of Runx2 obstructs the terminal differentiation of osteoblasts and increases bone resorption (Geoffroy et al.,2002 & Liu et al.,2001). These data suggest that tightly regulated Runx2 expression is essential for osteoblast differentiation from mesenchymal precursors.

Bone Morphogenetic Proteins (BMPs) and Wnt pathways are also essential for the early stages of osteoblastogenesis (Capulli et al., 2014).

The functions of osteoblasts include bone matrix synthesis and deposition of organic matrix and control of mineralization. Osteoblasts also regulate osteoclastogenesis to ensure correct bone mass and the proper balance between bone resorption and formation. Multiple mechanisms achieve this phenomenon. Critical among these is paracrine cross-talk between osteoblasts and osteoclasts utilizing Macrophage-Colony Stimulating Factor (M-CSF) (Felix et al., 1990).

Osteoblasts can have three possible fates. They can undergo apoptosis, become an osteocyte trapped within the matrix, or become a bone-lining cell (Capulli et al., 2014). The bone-lining cells are flat shaped osteoblast-derived cells that cover the bone surface and facilitate interaction between osteoclasts and bone matrix (Capulli et al., 2014). Recent studies have demonstrated the importance of Spindle-shaped N-cadherin Osteoblasts (SNO) on the endosteal surface of the bone. These cells increase osteoblast numbers by expressing regulatory molecules and activating regulatory pathways (Varnum-Finney et al., 2000).

1.4 Osteocyte

Osteocytes comprise most of the bone cells: They are also the most long lived bone cells with a life span that can reach 25 years. The osteocytes are connected by long and branched cellular processes that extend into connecting channels called canaliculi (Capulli et al., 2014). They connect through gap junctions that act as cell-to-cell communication portals.

Osteocytes have many functions, one of which is mechanosensing. They detect mechanical tension on the bone and translate that into biomechanical signaling (Capulli et al., 2014). Another function of the osteocyte is regulation of osteoclast behavior. Osteocytes can undergo apoptosis, which leads to an increase in RANKL that activates bone resorption through osteoclast differentiation and aggregation. Elevated levels of RANKL are associated with an increased number of osteoclasts (Noble et al., 2003).

All of these cells (osteoclast, osteoblast, and osteocyte) are vital for successful dental treatment. For example, orthodontic tooth movement depends on interactions between these cells to control the response to mechanical forces (Bumann & Frazier-Bowers, 2017). Previous studies also indicated that orthodontic loading affected osteocyte apoptosis (Kassem et al., 2017).

1.5 Periodontal Ligament

The periodontal ligament (PDL) plays an interesting and important role in wound healing: The PDL attaches the root of a tooth to an alveolar bone (Bosiakov et al., 2015). The PDL is made up of collagen fibers and a matrix that has nerve endings and blood vessels (Bosiakov et al., 2015). The PDL works not only as an attachment and support but also ensures proper bone reactions. This means that effects on the PDL can lead to bone reconstruction (Bosiakov et al., 2015). Stretching of the PDL leads to bone resorption while compression leads to bone formation (Bourauel et al., 2000). The importance of the PDL has led to studies of ways to regenerate it (Han et al., 2014). Multiple approaches have been undertaken in which bone marrow derived stem cells are used to as a basis for PDL

regeneration (Han et al., 2014). The PDL itself houses PDL stem cells (PDLSCs). They are, however, found in very small numbers (Maeda et al., 2013).

1.6 Embryological and tissue engineering concepts for regenerative medicine

Advances in embryology and tooth biology have led to advances in tissue engineering leading to new dental treatments. Implant-supported prosthetic dental reconstructive techniques have been improved. However, there are limitations in function and longevity due to alveolar bone loss (Catón et al., 2011). For example, natural teeth have plasticity from cementum and biological interaction with the alveolar bone through the PDL, while implants lack these functions.

The bioengineering approach to PDL has addressed this problem as a new treatment modality between diseased periodontium with implants or natural teeth (Taba et al., 2005). Tissue engineering utilizing stem cells is one of the candidates for a new therapy for damaged tissue (Xu et al., 2018). Recent studies also have focused on tooth biology regarding essential transcription factors, including bone morphogenic protein BMP2 & 4 and fibroblast growth factor FGF8. These molecules are believed to orchestrate signal transduction in tooth development that may lead to new treatment modalities (Neubüser et al., 1997; Catón et al., 2011).

1.7 Osseointegration

In modern dental implantology, the concept of "osseointegration", initially introduced by Professor Per-Ingvar Brånemark, is of paramount importance (Brånemark et al., 1969; Alifarag et al., 2018). In the clinic, osseointegration is responsible for permanent anchorage of titanium materials (e.g., dental implants and artificial limbs) to the human skeleton. This

phenomenon is based on the ability of human bone cells to attach to a metal surface, defined as "a direct connection between living bone and a load-carrying endosseous implant at the light microscopic level" (Brånemark et al., 2005).

1.8 Primary stability in dental implant

Primary stability at the time of the insertion of the implant relies on the physical interaction between bone and the implant (Lahens et al., 2016). It is essential to have excellent primary stability to avoid any implant micro-movement.

Secondary stability is related to the speed of bone remodeling and its extent around the implant: It is key to implant success and is affected by many factors (Albrektsson et al., 1981). Adequate bone density at the implant site is vital for implant success (Marquezan et al., 2012). This systematic review found a strong positive association between the primary stability of the implant and bone mineral density.

Another critical factor is the surgical technique for implant site preparation (Trisi et al., 2016a). The geometry of the post-insertion is directly related to implant success. High insertion torque (>25 Ncm, up to 176 Ncm) significantly increased bone-to-implant contact percentage as assessed by implant micro-mobility (Trisi et al., 2009).

Friction between the implant and the bone walls improves primary stability (Trisi et al., 2016a). With increased friction and improved primary stability, osseointegration leads to new bone on the implant surface, allowing secondary stability.

Anatomical factors that can affect osseointegration include sparse bone mineral density (BMD), and maxillary alveolar bone in which placed implants have less primary and secondary stability (Trisi et al., 2016a).

1.9 Osseodensification

Implant dentistry mainly developed by relying on material science to develop implant body materials and surface compositions. However, biocompatible titanium alloy does not guarantee osseointegration (Lopez et al., 2017).

Different techniques for preparation of an implant osteotomy may lead to different bone healing outcomes. For example, insufficient bone volume is a common problem in the edentulous posterior maxillae. In this case, sinus floor elevation with an osteotome is a standard approach allowing placement of longer implants in an ideal axial orientation. This technique is termed bone-added osteotome sinus floor elevation (BAOSFE) technique (Summers, 1994). However, the osteotome technique is a traumatic procedure; The instruments compact and expand the bone by the explosive percussive impact of a surgical mallet.

Recently, a novel concept "osseodensification" increases the quantity and density of bone surrounding implants without traumatic impact by creating compacted bone with a particular thread designed non-subtractive drilling called Densah bur ™ (**Figure 1**) (Huwais S. Fluted osteotome and surgical method for use. Patent No.: US 9,028,253 B3, May 12, 2015).

Figure 1. The geometric configuration of osteotomy drills

These CAD images illustrate geometric configuration of (a) conventional osteotomy bur

and (b) Densah bur™. Reprinted from Journal of Orthopaedic Research, Volume: 36,

Issue: 9, Pages: 2516-2523, First published: 14 March 2018, DOI: (10.1002/jor.23893)

Osseodensification is a novel bio-mechanical site preparation technique that produces low

plastic deformation leading to preservation of the bone and enhances the host bio-reaction.

The osseodensification technique is classified as a non-extraction technique due to

preserving bone by condensing bone. Conventional standard drilling techniques is

classified as an extraction technique due to removing bone while drilling (Huwais and

Meyer, 2017).

In a meta-analysis of different drilling techniques, the osseodensification bur significantly

reduced alveolar crest loss (Tretto et al., 2018). The bone temperature was higher in the

osseodensification compared to the conventional osteotomy group; it was still below the 27°C threshold for thermal necrosis (Huwais et al., 2017; Tretto et al., 2018).

The ideal rotational speed of the Densah bur is 800 to 1500 revolution per minute (RPM) with sufficient irrigation to prevent bone overheating (Trisi et al., 2016a). This bur has two different functions depending of the direction of rotation counterclockwise utilizes four tapered flutes with a negative rake angle to create a layer of compact / dense bone while clockwise rotation utilizes a positive rake angle and extracts bone as in conventional osteotomy (Lahens et al., 2016).

When rotated counterclockwise, non-cutting direction in densifying mode, downward pressure with adequate external irrigation creates a gentle compression wave inside the osteotomy along the fluted structure. This hydrodynamic process generates a densified layer through compaction with autogenous bone remnant as an autografting material derived from the surrounding bone. This creates a plastically expanded bony ridge (Meyer and Huwais et al.,2014; Oliveira et al., 2018).

This technique condenses bone leading to increased peri-implant bone density which is essential for implant success (Trisi et al., 2016a). The drill design increases the initial primary stability by densifying bone in the surrounding wall after osteotomy (Jimbo t al., 2014).

A sheep ilium study examined the primary stability of endosteal dental implants. The osseodensification procedure showed abundant bone remnants surrounding the implant surface with a higher insertion torque level. Conventional osteotomy rarely found bone remnants. (Lahens et al., 2016). The Osseodensification technique produced higher bone-

to-implant contact (BIC), regardless of implant macrogeometry. The higher BIC was obtained from histomorphometric analysis, and represents stronger implant stability; A high BIC level has a higher chance of implant success (Stokholm et al., 2014).

A recent study indicated that the autogenous bone remnants left by osseodensification facilitated the bridge between native bone and implant gap. These acted as nucleating sites for osteoblastic bone deposition in the adjacent bone along the implant surface. Conventional osteotomy did not show this phenomenon. The compacted bone remnant by osseodensification facilitates the bridging of new bone between the native bone (as a recipient) and implant (as a donor) during osseointegration (Alifarag et al., 2018). This observation may explain why osseodensification improves the secondary stability of implants.

We strongly agree with the following statements: As osseodensification is a newer technique, there is less clinical evidence to support it; nevertheless, early animal studies show promise for increasing dental implants' success (Tretto et al., 2018).

1.10 Hypotheses and Aims

We hypothesized that proper manipulation of the recipient site induces cellular activities to accelerate new bone formation. In this study, we investigated bone formation within the surgically created critical defect by the osseodensification method compared with regular osteotomy under ex-vivo calvaria static organ culture conditions.

CHAPTER 2

MATERIALS AND METHODS

2.1 Mice Calvaria

Boston University Institutional Animal Care and Use Committee (IACUC) approved the following experiment (AN-14946: Studies of factors that affect bone remodeling in ex-vivo neonatal mouse calvarial bone organ cultures). A total of 15 Calvaria dissected from 7-9 days old neonatal CD-1 mice (Charles River Laboratories, MA) under sterile conditions were trimmed and cut in half through the midsagittal suture halving the occipital lobe and between the two frontal lobes (**Figure 2-3**). Calvaria then was rinsed with culture medium before each half being placed in individual wells of six-well plates (Sigma Aldrich) over a stainless-steel mesh with 2.0 ml of culture medium. The tissue was incubated at 37°C and 5% CO_2.

Figure 2. Harvesting Calvaria

15 neonatal mice were euthanized and soft tissue removed prior to harvesting calvaria under sterile conditions.
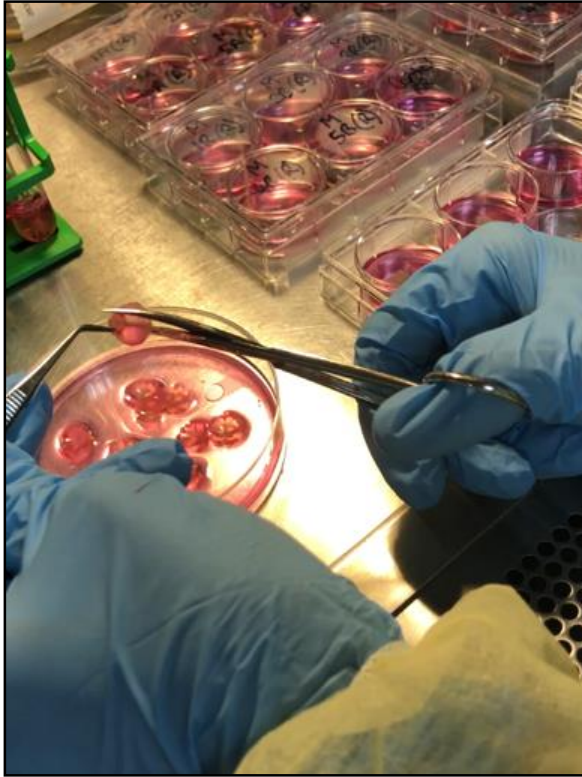
Figure 3. Calvarial Dissection into Right and Left Halves

Harvested Calvaria were then dissected along the sagittal suture into right and left halves.

2.2 Ex-Vivo Organ Culture

The harvested calvaria was cultured with an osteoblast activating medium. The calvaria organ culture medium was Dulbecco's Modified Eagle Medium (DMEM, Sigma-Aldrich) supplemented with 1% Penicillin-streptomycin solution, 5% (5mg/ml) Bovine Serum Albumin (BSA), and (150µg/ml) ascorbic acid (Sigma-Aldrich) instead of Fetal Calf Serum. The media was exchanged every other day.

Our previous study had determined that the lack of fetal calf serum (FCS) allowed for precise observation of the effect of the added factors: The osteoblast directed bone

13

formation or osteoclast directed bone resorption (Bone Research Protocols Third Edition;

Aymen I. Idris Editor, Chapter 11: Ex vivo Models of Cancer-Bone Cell Interaction, p221-

224). The additional supplement of ascorbic acid induces the bone formation phase that

primes osteoblast to synthesize collagen.

2.3 Surgical Defect

A critical size defect is defined as a defect that does not heal spontaneously without a

scaffold. A previous study showed that a 2mm diameter defect was a crucial size in

neonatal mice (Wu X, Downes S, Watts DC. Evaluation of critical size defects of mouse

calvarial bone: An organ culture study. Microsc Res Tech. 2010;73(5):540-547). We

created a 2mm diameter defect in each calvaria half by a low-speed handpiece.

We surgically created a 0.5mm pin-hole in the center of the right side of the parietal bone

as a guide for the osteotomy.

2 mm diameter Densah burs with a low speed rotation at 500 revolutions per minute (RPM)

created approximately 2 mm diameter of critical defect.

The left half underwent conventional osteotomy by a clockwise direction in order to create

a non-compressed bone-edge as a control group. In contrast, the right half of each calvaria

underwent osseodensification in a counter-clockwise direction in order to create a

compressed bone-edge as a test group (**Figures 3 & 4**).

After the osteotomy, each calvaria was stationed on the triangular stainless grid that

provides organs as a floating condition in the 6-well culture plate with 2ml of the bone

formation medium described above (**Figure 5**). The endocranial/concave side bathes in

the media, and the exocranial surface is partially exposed above the medium (Trowell,

1954). Five calvaria halves were cultured in each 6-well plate, and the remaining well contained only medium as an indicator of contamination as well as a control for the biological evaluation. Tissues were incubated at 37°C with 5% CO_2 and medium exchanged every two days. Spent medium were transferred to individual tubes and snap-frozen and stored at -80°C to determine alkaline phosphatase (ALP) activity. Five control and test calvaria were harvested after 7, 14 or 28 days and fixed with 2 ml of 4% formaldehyde in glass sample tubes at 4°C for 48 hours and kept in 70% ethanol at 4°C for histological analysis.

Figure 4: Osteotomy on the calvaria by the Densah™ bur
The osteotomy was performed utilizing a 2mm diameter of the Densah™ bur with 500 rotation speed per minute under sterile conditions.

Figure 5: Calvaria on Top of a Triangular Stainless-Steel Metal Grid in Each Well

Five calvaria halves were cultured in each 6-well plate. The remaining well contained medium only as an indicator of medium contamination. The calvaria were incubated at 37°C with 5% CO_2 and medium was changed every two days.

2.4 Sample Collection

It was challenging to evaluate microscopic image analysis during the organ culture due to the unclear view with the metal mesh as an obstruction. The edge of the calvaria could not detach because of physical attachment to the stainless-steel mesh. Thus, samples were fixed in formalin and detached from the mesh before microscopy image analysis at post-operative day 7, 14 and 28 as shown on the **Table 1**.

Group Name	Culture Duration	Right Halves: Osseodensification	Left Halves: Conventional Osteotomy
Group A	7 days culture	N=5	N=5
Group B	14 days culture	N=5	N=5
Group C	28 days culture	N=5	N=5

Table 1. Experimental Group

Three different groups: cultured for 7, 14, or 28 days were designated as Group A, B, and C, respectively.

2.5 Morphological Analysis

We then assessed the morphological change of calvaria defect by microscopy image analysis on day 7, day 14, and day 28, as an early post-operative phase (group A), intermediate phase (group B), and late phase (group C), respectively (**Table 1**). We took microscopic photos utilizing the 2 mm grid plate superimposing, each photo was converted into Image J to evaluate the defect closure, by tracing the outline of the original defect and current defect size, and generated graphs by Microsoft Excel and following statistical analyses.

2.6 Biological Analysis

Alkaline phosphatase (ALP) is an enzyme secreted by osteoblasts and used as a marker for bone metabolism. A high level of ALP activity, as a byproduct of osteoblast activity, provides essential information into the fundamental mechanisms of hard tissue formation (Golub et al., 2007Golub et al., 2007). ALP enzyme secretion was measured following the protocol of the TRACP & ALP Assay Kit (Cat #MK301, Takara Bio Inc.).

17

2.7 Statistical Analysis

In this study, SPSS25 software was used for statistical data analysis, including descriptive statistical analysis of all three groups. The Shapiro-Wilk test was used to assess the normality of continuous variables, and calculated means of both the control group (Conventional osteotomy) and the test group (densified osteotomy) with standard deviations. The student t-test assessed statistically significant differences between two groups with the two-tailed p-value of < 0.05 as statistically significant. Trends were calculated using SPSS to check for changes across time intervals. Figures were generated using Microsoft Excel. We also assessed the association between time intervals among the control and the test group for statistical significance using a student t-test.

CHAPTER 3

RESULTS

3.1 Aim: Osseodensification induced morphological change by increased cellular migration and proliferation

3.1.1 Microscopic image collection

The photomicrographic analyses are illustrated in **Figures 6 and 7**. Each calvaria was fixed with 4% formaldehyde for 48 hours and stored in 70% EtOH at 4°C as described in the materials and methods.

Figure 6 shows the morphological changes of defect closure from postoperative day 7 to 28 as the "control group" with conventional osteotomy mode. There was minimal cellular migration or proliferation toward the defect area from the bone side.

A.

B.
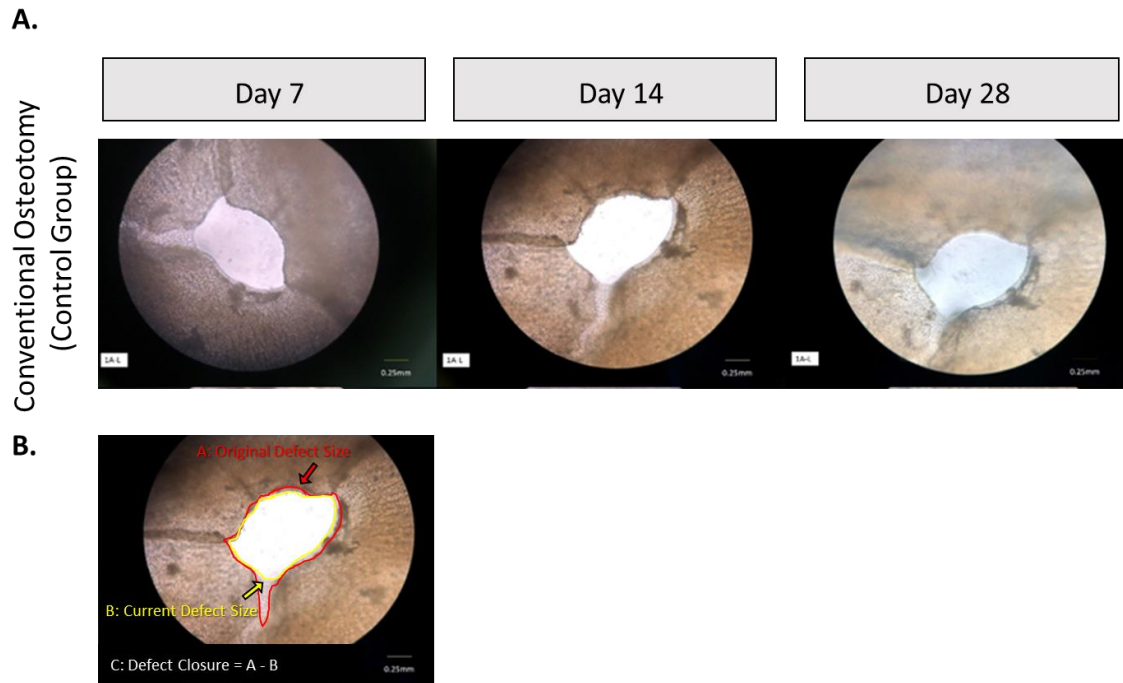
Figure 6. Microscopic Image Analysis of the Control Group Defect over time (Left Halves of Calvaria, Conventional Osteotomy)

A. Each row shows images from calvaria harvested and photographed at day 7, 14, and 28 respectively. There was minimal decrease in the size of the defect from day 7 to day 28.

B. These qualitative images were taken to visually inspect the progression of the defect closure over the study duration. Visual tracing using Image J was used to create quantitative data from these images.

Figure 7 shows morphological changes of defect closure from postoperative day 7 to 28 as the "test group" with compressed osteotomy (osteocondensification mode) from the Densah™ bur. The cellular migration or proliferation increased toward the defect area from the edge of the defect.
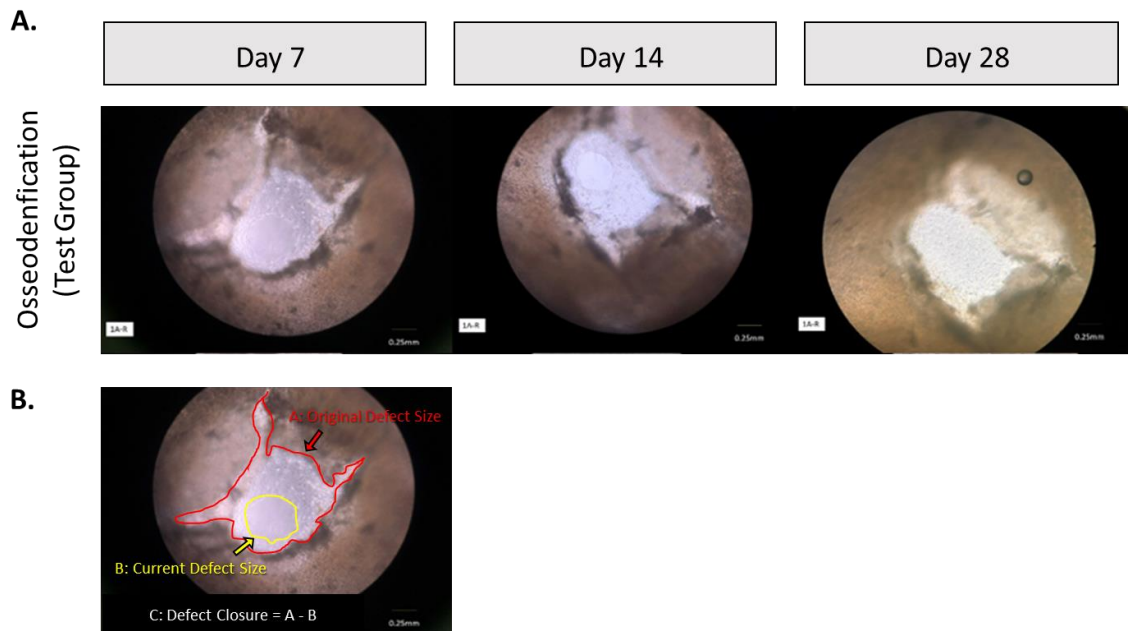
Figure 7. Microscopic Image Analysis of the Osseodensification Group Defect Closure over time (Right Halves of Calvaria)

A. Test Group: Each row shows defect size in calvaria harvested and photographed at day 7, 14, and 28.

B. These qualitative images were taken to visually inspect the progression of the defect size over the study duration. Visual tracing using Image J was used to create quantitative data from these images.

21

3.1.2 Statistical Analysis of Defect Size

The statistical analysis of defect size created by Image J software on a standardized scale (0.25mm) is shown in **Figures 6 & 7**. This image analysis allows evaluation of the progression of defect closure quantitatively over the study duration (**Table 2-10**).

Each table represents the morphological change by the "original defect size" (mm^2) at the day of the osteotomy (day 0), "current defect size" (mm^2) at the indicated post-operative days (**Table 2-10**). The current defect size was subtracted from the original defect size to determine "defect closure size" (mm^2). The mean value, the standard deviation of the mean, and the standard error of the mean are shown for each category (n=5).

Table 2 compared "original defect size" between the control group and the test group. According to the Shapiro-Wilk W test, the control group showed normal distribution. However, the test group showed non-normal distribution. The Mann-Whitney U test, also called a Wilcoxon test, was used for statistical analysis between groups. There were no significant differences between groups (n=15, two-tailed probability = 0.1249).

Group A-C	Original Defect (Day 0)	
Sample	Control Group (Conventional)	Test Group (Densah)
1A	1.458	1.194
2A	1.642	1.448
3A	1.380	1.277
4A	1.579	0.973
5A	1.284	0.768
1B	2.221	2.894
2B	1.707	1.929
3B	1.474	1.189
4B	2.047	0.989
5B	1.072	0.938
1C	0.691	1.119
2C	1.426	1.631
3C	0.997	1.201
4C	1.346	1.271
5C	1.624	1.432
Average	1.463	1.350
SD	0.384	0.516

Table 2. Original Defect Size

There was no significant difference of original defects between groups.

Table 3 shows the early phase of morphological change in Group A after seven days culture. Both groups showed normal distribution in each parameter as "current defect" and "defect closure".

The osseodensification mode (test group), had significantly reduced "current defect size" at day 7 (0.883 ± 0.283 mm^2) compared to the conventional osteotomy mode (control group, 1.361 ± 0.163 mm^2), as shown by the Student t-test with a two-tailed probability value of 0.016.

However, the mean value of the "defect closure size" in the test group (0.249 ± 0.155 mm^2) was not significantly different from the control group (0.107 ± 0.085 mm^2), with a two-tailed probability value of 0.123 by Student t-test.

23

The mean value of the "original defect size" in the test group (1.132 ± 0.266 mm^2) was significantly smaller than the control group (1.469 ± 0.145 mm^2), with a two-tailed probability value of 0.046 by Student t-test.

Group A	Original Defect at Day 0 (mm^2)		Defect Size at Day 7 (mm^2)		Defect Closure (Day 0 – Day7, mm^2)	
	Control Group (Conventional)	Test Group (Osseodensification)	Control	Test	Control	Test
1A	1.458	1.194	1.206	0.668	0.252	0.526
2A	1.642	1.448	1.536	1.250	0.106	0.198
3A	1.380	1.277	1.344	1.108	0.036	0.169
4A	1.579	0.973	1.520	0.793	0.059	0.180
5A	1.284	0.768	1.201	0.597	0.083	0.171
Average	1.469	1.132 *	1.361	0.883 *	0.107	0.249
SD	0.145	0.266	0.163	0.283	0.085	0.155
SEM	0.065	0.119	0.073	0.127	0.038	0.069

two tailed test p = 0.0462 two tailed test p = 0.0156 two tailed test p = 0.125
one tailed test p = 0.0231 one tailed test p = 0.0078 one tailed test p = 0.0613

Table 3. The early phase of morphological change in Group A after 7 days culture

Table 3 summarizes the defect sizes for slides of Group A fixed at day 7. The test group (Osseodensification) had greater defect closure (0.249 ± 0.155 mm^2) than the control group (conventional osteotomy, 0.107 ± 0.085 mm^2).

Table 4 shows the morphological change in Group B after fourteen days culture. As same as Group A, both groups showed the normal distribution in each parameter as "current defect" and "defect closure".

The Student t-test seems an osseodensification mode (test group) has slightly reduced defect size (current defect 0.966 ± 0.381 mm^2) than the conventional osteotomy mode (control group, 1.491 ± 0.375 mm^2) with a one-tailed probability value of 0.0298 by Student t-test (two-tailed p value = 0.0596).

There was no significant difference (a two-tailed P=0.3273 by Student t-test) in the "defect closure size" between the test and control group, 0.622 ± 0.817 mm^2 and 0.213 ± 0.087 mm^2, respectively.

No significant differences (a two-tailed P=0.7927 by Student t-test) were observed in the "original defect size" between the test and control group, 1.588 ± 0.831 mm^2 and 1.704 ± 0.458 mm^2, respectively.

Group B	Original Defect at Day 0 (mm^2)		Defect Size at Day 14 (mm^2)		Defect Closure (Day 0 – Day14, mm^2)	
	Control Group (Conventional)	Test Group (Osseodensification)	Control	Test	Control	Test
1B	2.221	2.894	1.916	0.813	0.305	2.081
2B	1.707	1.929	1.459	1.636	0.248	0.293
3B	1.474	1.189	1.284	0.910	0.190	0.279
4B	2.047	0.989	1.799	0.723	0.248	0.266
5B	1.072	0.938	0.997	0.749	0.075	0.189
Average	1.704	1.588	1.491	0.966 *	0.213	0.622
SD	0.458	0.831	0.375	0.381	0.087	0.817
SEM	0.205	0.372	0.168	0.171	0.039	0.365

two tailed test p = 0.7927   two tailed test p = 0.0596   two tailed test p = 0.3273
one tailed test p = 0.3963   one tailed test p = 0.0298   one tailed test p = 0.1636

Table 4. The mid phase of morphological change in Group B as 14 days culture
Table 4 summarizes the defect sizes for Group B fixed at day 14.

In **Table 5-7**, we demonstrated the three phases (early, intermediate, and late phase) of morphological change from Group C samples cultured for 28 days.

Table 5 shows the early phase of morphological change after seven days culture. The test group (osseodensification mode) has significantly different defect closure size (0.501 ± 0.267 mm^2) compared to control group (conventional osteotomy mode, 0.090 ± 0.034 mm^2) with a two-tailed p value of 0.0256 similar to Group A. There were no significant

25

differences in the "original defect size" between the test and control group, 1.331 ± 0.203 mm^2 and 1.217 ± 0.371 mm^2, respectively (a two-tailed P = 0.5684 by Student t-test).

Group C	Original Defect (Day 0)		Current Defect (Day 7)		Defect Closure (Day 0 – Day7)	
	Control Group (Conventional)	Test Group (Osseodensification)	Control	Test	Control	Test
1C	0.691	1.119	0.597	0.172	0.094	0.947
2C	1.426	1.631	1.369	1.075	0.057	0.556
3C	0.997	1.201	0.919	0.844	0.078	0.357
4C	1.346	1.271	1.271	0.944	0.075	0.327
5C	1.624	1.432	1.479	1.112	0.145	0.320
Average	1.217	1.331	1.127	0.829	0.090	0.501 *
SD	0.371	0.203	0.363	0.383	0.034	0.267
SEM	0.166	0.091	0.162	0.171	0.015	0.120

two tailed test p = 0.5684   two tailed test p = 0.2428   two tailed test p = 0.0256
one tailed test p = 0.2842   one tailed test p = 0.1214   one tailed test p = 0.0128

Table 5. The early phase of morphological change in Group C after 7 days culture
The following throughout the study to assess for changes in these variables at different time intervals in Group C. The original defect was slightly bigger in the test group. However, the defect closure in the test group (0.501 ± 0.267 mm^2) was significantly greater than the control group (0.090 ± 0.034 mm^2).

Table 6 shows the intermediate phase of morphological change after fourteen days culture. The defect closure in the test group (0.628 ± 0.254 mm^2) was significantly greater than the control group (0.107 ± 0.090 mm^2) with two-tailed probability value 0.0076 by Student t-test.

Sample A	Original Defect (Day 0)		Current Defect (Day 14)		Defect Closure (Day 0 – Day14)	
	Control Group (Conventional)	Test Group (Osseodensification)	Control	Test	Control	Test
1A	0.691	1.119	0.653	0.120	0.038	0.999
2A	1.426	1.631	1.276	0.870	0.150	0.761
3A	0.997	1.201	0.978	0.641	0.019	0.560
4A	1.346	1.271	1.259	0.829	0.087	0.442
5A	1.624	1.432	1.383	1.056	0.241	0.376
Average	1.217	1.331	1.110	0.703	0.107	0.628 *
SD	0.371	0.203	0.296	0.358	0.090	0.254
SEM	0.166	0.091	0.132	0.160	0.040	0.114

two tailed test p = 0.5684 two tailed test p = 0.0872 two tailed test p = 0.0076
one tailed test p = 0.2842 one tailed test p = 0.0436 one tailed test p = 0.0038

Table 6. The intermediate phase of morphological change in Group C as 14 days culture

Table 7 demonstrates the late phase of morphological change after twenty-eight days culture. The defect closure in the test group (0.661 ± 0.332 mm^2) has also significantly greater than the control group (0.112 ± 0.114 mm^2) with two-tailed probability value 0.0177 by Student t-test.

Sample A	Original Defect (Day 0)		Current Defect (Day 28)		Defect Closure (Day 0 – Day28)	
	Control Group (Conventional)	Test Group (Osseodensification)	Control	Test	Control	Test
1A	0.691	1.119	0.673	0.018	0.018	1.119
2A	1.426	1.631	1.380	0.739	0.046	0.892
3A	0.997	1.201	0.975	0.652	0.022	0.549
4A	1.346	1.271	1.103	0.915	0.243	0.356
5A	1.624	1.432	1.394	1.041	0.230	0.391
Average	1.217	1.331	1.105	0.673	0.112	0.661 *
SD	0.371	0.203	0.301	0.396	0.114	0.332
SEM	0.166	0.091	0.135	0.177	0.051	0.149

two tailed test p = 0.5684 two tailed test p = 0.0908 two tailed test p = 0.0177
one tailed test p = 0.2842 one tailed test p = 0.0454 one tailed test p = 0.0089

Table 7. The late phase of morphological change in Group C as 14 days culture

Figure 8 illustrated the time-dependent defect closure compared with the conventional osteotomy control group, and the osseodensification as the test group. The original surgical defect size at day 0 in the test group (1.331 ± 0.203 mm^2) was not significantly different compared to the control group (1.217 ± 0.371 mm^2), The defect size was significantly decreased in the test group compared to the control group at day 14 and 28, as p-value 0.044 and 0.046 by student-t test, respectively.

Defect Size in a Time-Dependent Manner
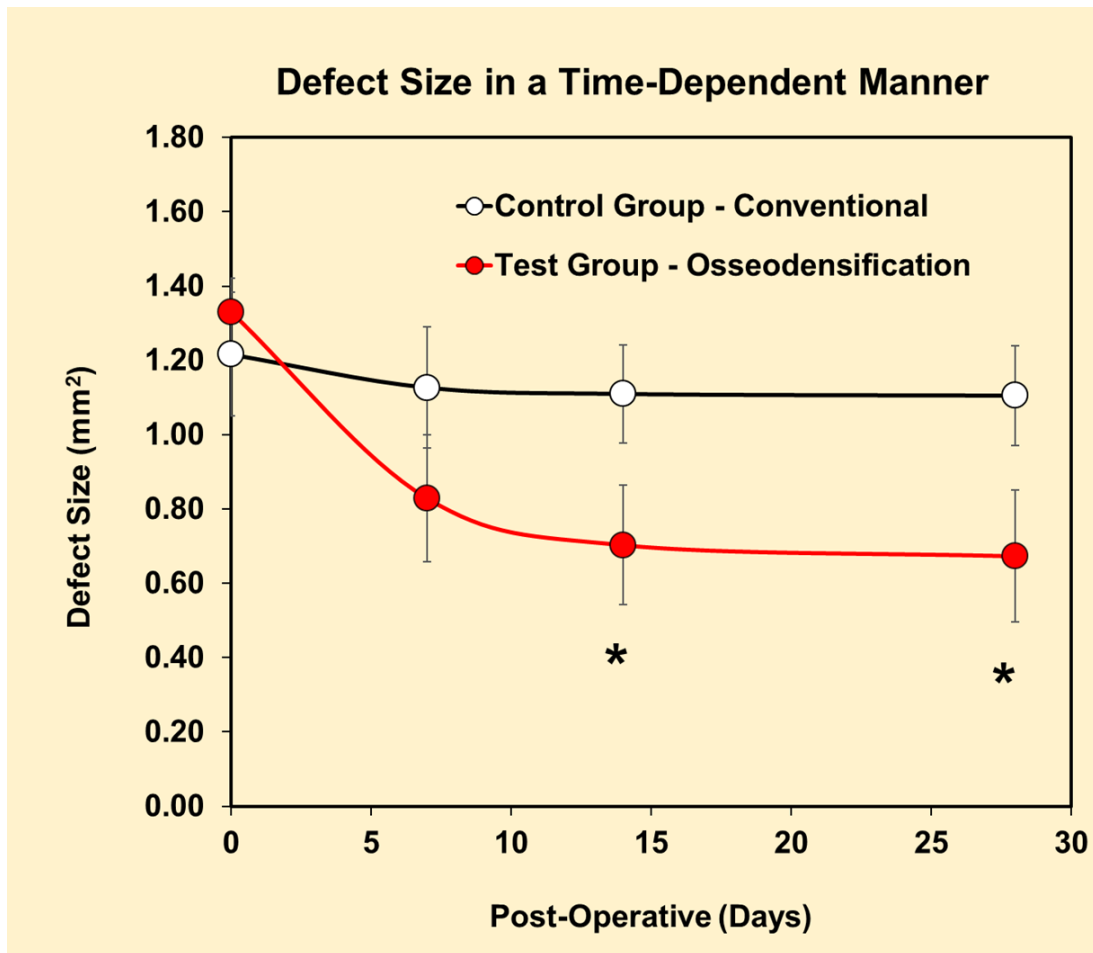
Figure 8. Timeline of current defect size in Group C comparing test group with control group

The graph shows the current defect size change throughout the study in Group C. The current defect was measured from visual tracing made by Image J on each slide to gain quantitative information. The current defect actually starts at a higher point for the Densah group due to the slightly bigger original defect in the test group. However, the current defect of the test group is significantly smaller and the defect has substantially more closure than the control group at day 14 and 28. *, $p<0.05$, *, $p<0.05$, one-way ANOVA and Turkey-Kramer HSD test, compared to control at each time-point.

Figure 9 illustrates the defect closure size, which calculated by subtracting the defect size at indicated time points (day 7, 14, 28) from the previous time point; e.g., subtracted the defect size at day seven from the defect size at day 0. **Table 8** also showed the statistical analysis of the defect closure size comparison between the test group and the control group. The test (osseodensification by Densah™ bur) group significantly improved healing, with greater defect closure caused by cellular migration and/or proliferation.

Cumulative Defect Closure in a Time-Dependent Manner
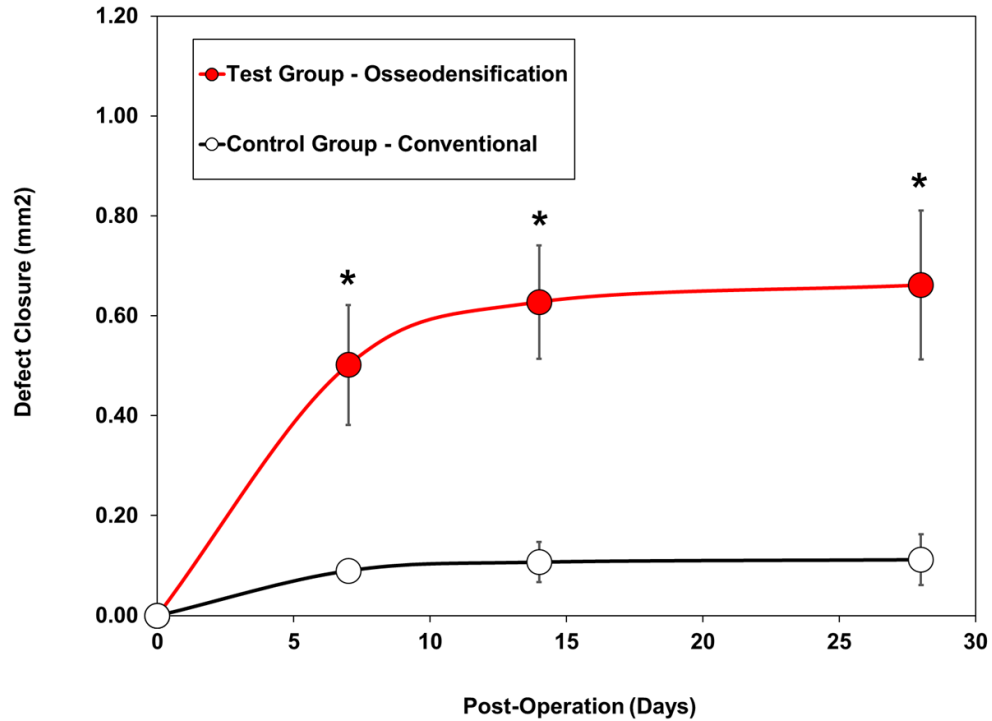
Figure 9. Cumulative defect closure in a time-dependent manner

The defect closure is measured as the remaining defect at each point in time subtracted from the original defect at the beginning of the study. In this timeline, the test group achieves significantly faster defect closure than the control group. *, $p<0.05$, one-way ANOVA and Turkey-Kramer HSD test, compared to control at each time-point.

We also analyzed defect closure size during the indicated period at Day 0-7, Day 7-14, and Day 14-28, as the early post-operative phase, the intermediate phase, and the late phase, respectively **(Figure 10).** Overall, the test group dramatically closed the surgical defect in the early post-operative phase and gradually reduced the closing ratio in the following

30

phases. In contrast, the control group did not accelerate in the early phase and persisted as low closing ratio than the test group.
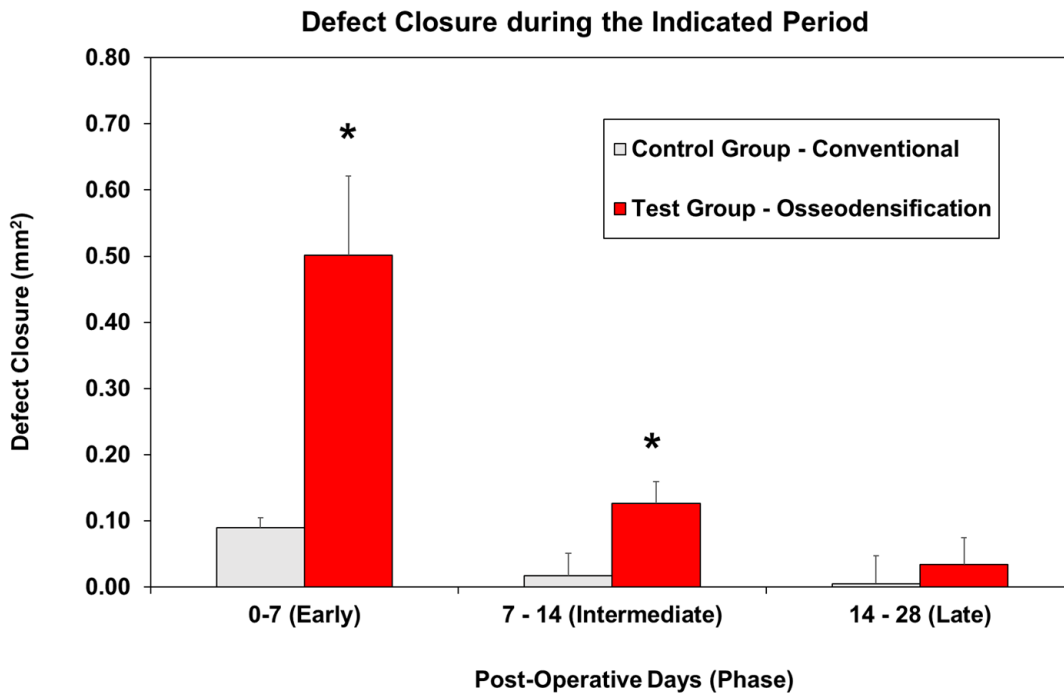
Figure 10. Defect closure during the indicated period

The graph indicates defect closure during the indicated period. Each defect closure (mm^2) is calculated by subtracting the defect closure of different points. The biggest change of defect closure was from day 0 to day 7 (early phase) in the test group. This is also evident in the other figures throughout this project. The test group seems to achieve high defect closure at the beginning of the study. In contrast, the control group has a slower rise in defect closure. The rise in defect closure in the conventional group is more of a trend without any significant landmark increases throughout the study. *, $p < 0.05$, Student t-test compared to control at each time-point.

Table 8 shows the defect closure size during indicated periods (day 0-7, day 7-14, and day 14-28). In the early post-operative phase (day 0-7), the test group indicated the defect was significantly covered by cells that migrate and/or proliferate than the intermediate (day 7-14) and late phase (day 14-28). For example, in the early phase (day 0-7) of the test group significantly closed the surgical defect compared to the intermediate phase (day 7-14, P=0.0110) and late phase (day 14-28, P=0.0024 by one-way ANOVA and Turkey-Kramer HSD test. However, there was no significant differences in the control group.

Control Group: Oneway Analysis of defect Closure by the indicated phase
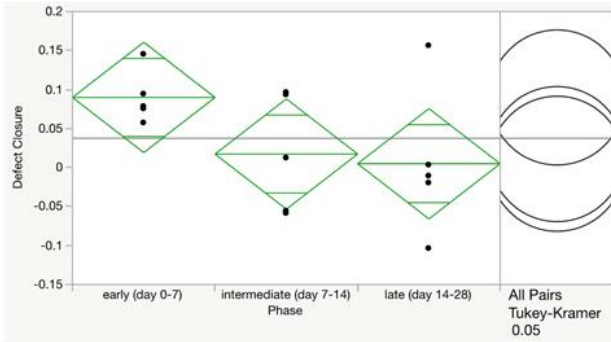
Summary of Fit

Rsquare	0.250104
Adj Rsquare	0.125122
Root Mean Square Error	0.072579
Mean of Response	0.037267
Observations (or Sum Wgts)	15

Analysis of Variance

Source	DF	Sum of Squares	Mean Square	F Ratio	Prob > F
Phase	2	0.02108253	0.010541	2.0011	0.1778
Error	12	0.06321240	0.005268		
C. Total	14	0.08429493			

Mean of Oneway ANOVA

Level	Number	Mean	Std Error	Lower 95%	Upper 95%
early (day 0-7)	5	0.089800	0.03246	0.0191	0.16052
intermediate (day 7-14)	5	0.017200	0.03246	-0.0535	0.08792
late (day 14-28)	5	0.004800	0.03246	-0.0659	0.07552

Ordered Differences Report

Level	- Level	Difference	Std Err Dif	Lower CL	Upper CL	p-Value
early (day 0-7)	late (day 14-28)	0.0850000	0.0459029	-0.037458	0.2074579	0.1950
early (day 0-7)	intermediate (day 7-14)	0.0726000	0.0459029	-0.049858	0.1950579	0.2906
intermediate (day 7-14)	late (day 14-28)	0.0124000	0.0459029	-0.110058	0.1348579	0.9607

Test Group: Oneway Analysis of defect Closure by the indicated phase
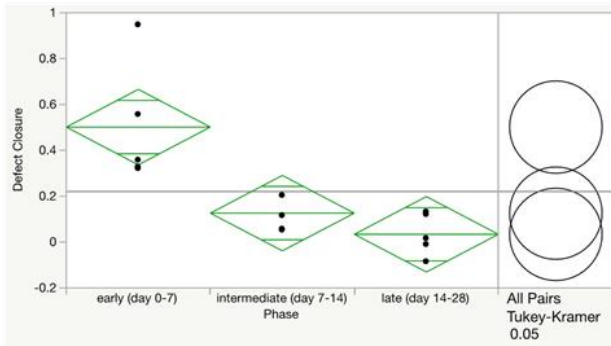
Summary of Fit

Rsquare	0.642006
Adj Rsquare	0.58234
Root Mean Square Error	0.168812
Mean of Response	0.220467
Observations (or Sum Wgts)	15

Analysis of Variance

Source	DF	Sum of Squares	Mean Square	F Ratio	Prob > F
Phase	2	0.61327093	0.306635	10.7601	0.0021*
Error	12	0.34197080	0.028498		
C. Total	14	0.95524173			

Mean of Oneway ANOVA

Level	Number	Mean	Std Error	Lower 95%	Upper 95%
early (day 0-7)	5	0.501400	0.07550	0.3369	0.66589
intermediate (day 7-14)	5	0.126200	0.07550	-0.0383	0.29069
late (day 14-28)	5	0.033800	0.07550	-0.1307	0.19829

Ordered Differences Report

Level	- Level	Difference	Std Err Dif	Lower CL	Upper CL	p-Value
early (day 0-7)	late (day 14-28)	0.4676000	0.1067662	0.182774	0.7524263	0.0024*
early (day 0-7)	intermediate (day 7-14)	0.3752000	0.1067662	0.090374	0.6600263	0.0110*
intermediate (day 7-14)	late (day 14-28)	0.0924000	0.1067662	-0.192426	0.3772263	0.6712

Table 8. Defect Closure in the indicated period

*, p<0.05 one-way ANOVA and Turkey-Kramer HSD test

CHAPTER 4

DISCUSSION

4.1 Role of Osseodensification

Osseodensification is a new surgical concept for biomechanical recipient site preparation for dental implant placement developed by Huwais (Huwais S. Enhancing implant stability with osseodensification: A two year follow up. Implant Pract 2015; 8: 28-34). The low plastic deformation of bone created by rolling and sliding contact using a densifying bur, called Densah™ bur, is the basics for this procedure. The low plastic deformation can maintain sufficient bone quantity and quality (density) in the implant recipient site. Thus, this approach leads to faster wound healing as the cells surrounding the defect can activate the healing cascade more quickly.

A standard osteotomy drill excavates bone and the osteotomes tend to result in trabecular fractures. This problem will lead to long remodeling time and postpone development of secondary stability of the implant. The Densah™ bur improves bone preservation and condensation by compression of the bone without fracture. This mechanical advantage increased the bone density at the cutting-edge and improved the mechanical stability of implants (Huwais S, Meyer E. Osseodensification: A novel approach in implant osteotomy preparation to increase primary stability, bone mineral density and bone to implant contact. Int J Oral Maxillofac Implants 2016; 32: 27-36).

Bone remodeling after conventional osteotomy requires approximately 3 months to reconstruct the damaged area by letting the strain reach or go beyond the threshold of micro damaged bone (Frost HM. A brief review for orthopedic surgeons: Fatigue damage

34

(microdamage) in bone (its determinants and clinical implications). J Orthop Sci 1998; 3: 272-81). These descriptions suggested that osseodensification will help preserve bone mass and increase density to shorten the healing period.

A previous study on femoral neck fractures established that stabilizing bones is extremely important for bone recovery (Samsami et al., 2015). Multiple explanations are available as to why static conditions improve bone healing, especially in the initial healing stage. Under static conditions, bone cells have a stable environment in which to proliferate and migrate to heal the defect. A static condition also results in less of a weight-bearing burden due to gravity or stress (Vetsch et al., 2016).

We created a stabilized bone remodeling condition with static organ culture status (Liedert et al., 2005). Wound healing starts with the proliferation phase in which angiogenesis and fibroplasia occur (Greaves et al., 2013). These with re-epithelization go to form the extracellular matrix and granulation tissue. Complex transcription factors play a role in this process. TGF-β has been singled out for its importance in wound healing. It stimulates collagen synthesis. However, increased levels of this factor were shown to delay wound healing (Kasuya and Tokura, 2014).

4.2 Osseoinduction

Osteoinduction is the process of osteogenesis, which is important in bone healing (Albrektsson and Johansson, 2001). The primitive undifferentiated pluripotent cells are stimulated to differentiate into bone-forming cells. These undifferentiated cells serve an essential role in bone healing. An inductive agent pushes these undifferentiated cells into proliferating and becoming bone cells (Albrektsson and Johansson, 2001). Local chemical

signals and messengers play essential roles in initiating this process as well. Osteoinduction is responsible for the majority of bone growth after injury. Hence, it could be the element that is most influenced by osseodensification.

4.3 Osseocondution

Osteoconduction is the process by which bone grows on a surface. The osteoconductive surface permits bone growth on top of it and into its pores. This process which helps the bone either grow on a static grid-like mesh or an implant surface is highly dependent on pre-existing osteoblasts. Bone growth factors, such as IGF-1, fibroblast growth factor (FGF), TGF-B and platelet-derived growth factor (PDGF) are signaling proteins that help in osteoconduction. These factors listed also have angiogenic properties, meaning they augment the growth of blood vessels (Albrektsson and Johansson, 2001).

4.4 Angiogenesis in bone healing process

Angiogenesis is a critical process for wound healing. It depends on the interplay between complex signaling molecules and messengers. Adhesion molecules, proteinases, cytokines, and chemokines, as well as growth factors all, play an integrated role in advancing this process (Greaves et al., 2013).

There have been many attempts to improve wound healing. With the recent discovery of the importance of signaling molecules and messengers, efforts to manipulate them have increased (Kasuya and Tokura, 2014). Inflammation is an essential process for optimal wound healing. Excess inflammation may delay the wound healing process because of prolonged edema and pro-inflammatory cytokines that are harmful to wound healing. We

believe that the effort to accelerate and improve wound healing will prove vital for implant success.

4.5 Tissue Engineering Concept

New treatment modalities to improve bone healing are also in development. Tissue engineering can be combined with osseodensification for example to utilize the body's healing mechanism (Suárez-González et al., 2014). Growth factors, such as vascular endothelial growth factor (VEGF) and beta-tricalcium phosphate (β-TCP), are part of the new approach to improve bone healing.

4.6 Implant Stability

Implant stability and osseointegration are of paramount importance when it comes to implant success (Coelho and Jimbo, 2014). Only a small number of studies have examined the effect of osseodensification on bone healing. This study assessed the effect and speed of mouse calvaria bone healing within a surgical defect. While the calvaria of mice does not have the typical low bone density that benefits most from the osseodensification our results still show statistical differences (Huwais and Meyer, 2017; Oliveira et al., 2018).

In comparison to the conventional method, osseodensification showed statistically significant faster bone healing that was. This result is in line with the literature showing that the osseodensification technique improves bone recovery (Coelho et al., 2013). Osseodensification improves bone recovery in part because of improved osseointegration (Huwais and Meyer, 2017).

4.7 Osseodensification induced cellular activity

Our results showed that bone growth started much earlier after an osseodensification induced effect in comparison to the conventional method. This phenomenon may be explained because the osseodensification technique creates osteotomes that preserve the bone cells at the site instead of creating a complete empty defect (Galli et al., 2015). The cells present at the osteotome site can start the healing cascade faster. This could explain why bone regeneration started at a much earlier time interval in the osseodensification group than the conventional group.

Osseodensification preserves the bone architecture around the defect by creating osteotomes. This approach was shown to increase bone density in the peri-implant area (Pai et al., 2018). Our results suggest that the faster healing achieved with the osseodensification bur could result in better healing in the peri-implant site.

Furthermore, Group C, the group that was followed up over different stages in the experiment offers valuable information regarding the trajectory of defect closure over time. As demonstrated in the result section the defect closure in the conventional group starts to pick up after day 7. However, it still trails the defect closure of the osseodensification group. Our hypothesis was the osteotomes created by the osseodensification technique lead to not just faster bone growth start but more regeneration over time (Alifarag et al., 2018; Summers, 1994). This was also supported that by the percent defect size, a measurement obtained from calculating the defect size change over time. Comparison of this measurement between the conventional and the osseodensification group showed a much more significant change in percent defect size.

Research in bone biology and healing has shown that different bone cells interact together to initiate bone resorption and growth (Capulli et al., 2014). Preservation of these bone cells and compaction could also lead to better gap junction communication between the cells to jump-start the healing process in the defect (Han et al., 2011).

The added benefit of faster better bone regeneration could be of particular value in sites with a low bone density such as the upper human jaw (Marquezan et al., 2012). The Osseodensification method leads to a higher bone volume and density at the site (Trisi et al., 2016b). These findings, combined with the results of this study showing faster bone regeneration at the site when the osseodensification technique is utilized further solidify the benefit of this technique for areas with sparse bone density.

4.8 Future approach

In the future, a more focused approach to osseodensification in research could be beneficial. Only a small number of studies have been done on this technique as it is a new development. Recent research has shown that different drilling techniques could lead to different healing outcomes which is why this process was initially developed.

The in-vivo experiment will provide us thorough understanding regarding this new technique. This study has shown that osseodensification induced bone healing by cellular migration and proliferation under the ex-vivo conditions. However, more extensive research on patients would be very informative. More exposure and training in this technique could lead to more utilization in cases where it is highly indicated such as in areas with sparse bone density where osseodensification has shown to be superior to other techniques in many studies.

A follow-up study on our project could be done with a bigger sample size. A more thorough follow up timeline could uncover where osseodensification is most beneficial. According to our study, osseodensification leads to better bone recovery in the very early phase. We expect future research will evaluate the mechanism of osseointegration regarding the dental implant success rate that will benefit patients who needs implant placement.

CHAPTER 5

CONCLUSION

Osseodensification is a rising surgical technique that has been recently developed to improve both primary and secondary implant stability leading to improved dental implant success. Our results suggested that the osseodensification method induced cellular migration and proliferation toward the defect area in comparison to conventional drilling techniques. This phenomenon may indicate the induction of the essential host response for the wound healing process.

Many reasons could account for this change. The previous study has shown that osseodensification leads to better bone density in the peri-implant site with more intact or activated cells around the bone defect that could lead to faster activation of the healing cascade. Furthermore, these cells may release more essential healing mediators such as angiogenic and growth factors.

We believe that future studies to target patients utilizing the osseodensification drills to assess both primary and secondary implant stabilities and wound healing could more reliably showcase the importance of this novel drilling technique.

BIBLIOGRAPHY

1. Albrektsson, T., Brånemark, P.I., Hansson, H.A., Lindström, J., 1981. Osseointegrated titanium implants. Requirements for ensuring a long-lasting, direct bone-to-implant anchorage in man. Acta Orthopaedica Scandinavica. 52, 155–170.

2. Albrektsson, T., Johansson, C., 2001. Osteoinduction, osteoconduction and osseointegration. European spine journal. Off. Publ. Eur. Spine Soc. Eur. Spinal Deform. Soc. Eur. Sect. Cerv. Spine Res. Soc. 10 Suppl 2, S96-101.

3. Alifarag, A.M., Lopez, C.D., Neiva, R.F., Tovar, N., Witek, L., Coelho, P.G., 2018. Temporal osseointegration: Early biomechanical stability through osseodensification. The Journal of Orthopaedic Reseach. https://doi.org/10.1002/jor.23893

4. Bosiakov, S.M., Koroleva, A.A., Rogosin, S.V., Silberschmidt, V.V., 2015. Viscoelasticity of periodontal ligament: an analytical model. Mechanics of Advanced Materials and Modern Processes. 1. https://doi.org/10.1186/s40759-015-0007-0

5. Bourauel, C., Vollmer, D., Jäger, A., 2000. Application of bone remodeling theories in the simulation of orthodontic tooth movements. The Journal of Orofacial Orthopedics. 61 (4) , 266–279.

6. Bumann, E.E., Frazier-Bowers, S.A., 2017. A new cyte in orthodontics: Osteocytes in tooth movement Orthodontics Craniofacial Research. 20 Suppl 1, 125–128. https://doi.org/10.1111/ocr.12176

7. Capulli, M., Paone, R., Rucci, N., 2014. Osteoblast and osteocyte: Games without frontiers. Archives of Biochemistry and Biophysics, Bone: A dynamic and integrating tissue 561, 3–12. https://doi.org/10.1016/j.abb.2014.05.003

8. Catón, J., Bostanci, N., Remboutsika, E., De Bari, C., Mitsiadis, T.A., 2011. Future dentistry: cell therapy meets tooth and periodontal repair and regeneration. Journal of Cellular and Molecular Medicine. 15, 1054–1065. https://doi.org/10.1111/j.1582-4934.2010.01251.x

9. Coelho, P.G., Jimbo, R., 2014. Osseointegration of metallic devices: current trends based on implant hardware design. Archives of Biochemistry and Biophysics, Bone. 561, 99–108. https://doi.org/10.1016/j.abb.2014.06.033

10. Coelho, P.G., Marin, C., Teixeira, H.S., Campos, F.E., Gomes, J.B., Guastaldi, F., Anchieta, R.B., Silveira, L., Bonfante, E.A., 2013. Biomechanical evaluation of undersized drilling on implant biomechanical stability at early implantation times. Journal of Oral and Maxillofacial surgery. Off. J. Am. Assoc. Oral Maxillofac. Surg. 71, e69-75. https://doi.org/10.1016/j.joms.2012.10.008

11. Felix, R., Cecchini, M.G., Hofstetter, W., Elford, P.R., Stutzer, A., Fleisch, H., 1990. Impairment of macrophage colony-stimulating factor production and lack of resident bone marrow macrophages in the osteopetrotic op/op mouse. Journal of bone and mineral research. Off. J. Am. Soc. Bone Miner. Res. 5, 781–789. https://doi.org/10.1002/jbmr.5650050716

12. Galli, S., Jimbo, R., Tovar, N., Yoo, D.Y., Anchieta, R.B., Yamaguchi, S., Coelho, P.G., 2015. The effect of osteotomy dimension on osseointegration to resorbable media-treated implants: a study in the sheep. Journal of Biomaterials. Appl. 29, 1068–1074. https://doi.org/10.1177/0885328214553958

13. Greaves, N.S., Ashcroft, K.J., Baguneid, M., Bayat, A., 2013. Current understanding of molecular and cellular mechanisms in fibroplasia and angiogenesis during acute wound healing. Journal of Dermatological Science. 72, 206–217. https://doi.org/10.1016/j.jdermsci.2013.07.008

14. Han, J., Menicanin, D., Gronthos, S., Bartold, P.M., 2014. Stem cells, tissue engineering and periodontal regeneration. Australian Dental Journal. 59 Suppl 1, 117–130. https://doi.org/10.1111/adj.12100

15. Han, Y., Jin, Y.-H., Yum, J., Jeong, H.-M., Choi, J.-K., Yeo, C.-Y., Lee, K.-Y., 2011. Protein kinase A phosphorylates and regulates the osteogenic activity of Dlx5. Biochemical and Biophysical Research Communications. 407, 461–465. https://doi.org/10.1016/j.bbrc.2011.03.034

16. Huwais, S., Meyer, E.G., 2017. A Novel Osseous Densification Approach in Implant Osteotomy Preparation to Increase Biomechanical Primary Stability, Bone Mineral Density, and Bone-to-Implant Contact. The International Journal of Oral and Maxillofacial Implants. 32, 27–36. https://doi.org/10.11607/jomi.4817

17. Jimbo, R., Tovar, N., Marin, C., Teixeira, H.S., Anchieta, R.B., Silveira, L.M., Janal, M.N., Shibli, J.A., Coelho, P.G., 2014. The impact of a modified cutting flute implant design on osseointegration. The International Journal of Oral & Maxillofacial Surgery. 43, 883–888. https://doi.org/10.1016/j.ijom.2014.01.016

18. Kassem, H.E., Talaat, I.M., El-Sawa, A., Ismail, H., Zaher, A., 2017. Orthodontically induced osteocyte apoptosis under different force magnitudes in rats: an immunohistochemical study. The European Journal of Oral Sciences. 125, 361–370. https://doi.org/10.1111/eos.12366

19. Kasuya, A., Tokura, Y., 2014. Attempts to accelerate wound healing. The Journal of Dematological Science 76, 169–172. https://doi.org/10.1016/j.jdermsci.2014.11.001

20. Lahens, B., Neiva, R., Tovar, N., Alifarag, A.M., Jimbo, R., Bonfante, E.A., Bowers, M.M., Cuppini, M., Freitas, H., Witek, L., Coelho, P.G., 2016. Biomechanical and histologic basis of osseodensification drilling for endosteal implant placement in low density bone. An experimental study in sheep. The Journal of the Mechanical Behavior of Biomedical Materials. of . 63, 56–65. https://doi.org/10.1016/j.jmbbm.2016.06.007

21. Liedert, A., Kaspar, D., Augat, P., Ignatius, A., Claes, L., 2005. Mechanobiology of Bone Tissue and Bone Cells, in: Kamkin, A., Kiseleva, I. (Eds.), Mechanosensitivity in Cells and Tissues. Academia, Moscow.

22. Lopez, C.D., Alifarag, A.M., Torroni, A., Tovar, N., Diaz-Siso, J.R., Witek, L., Rodriguez, E.D., Coelho, P.G., 2017. Osseodensification for enhancement of spinal surgical hardware fixation. The Journal of the Mechanical Behavior of Biomedical Materials. 69, 275–281. https://doi.org/10.1016/j.jmbbm.2017.01.020

23. Maeda, H., Fujii, S., Tomokiyo, A., Wada, N., Akamine, A., 2013. Periodontal tissue engineering: defining the triad. The International Journal of Oral & Maxillofacial Implants. 28, e461-471.

24. Marquezan, M., Osório, A., Sant'Anna, E., Souza, M.M., Maia, L., 2012. Does bone mineral density influence the primary stability of dental implants? A systematic review. Clinical Oral Implants Research. 23, 767–774. https://doi.org/10.1111/j.1600-0501.2011.02228.x

25. Noble, B.S., Peet, N., Stevens, H.Y., Brabbs, A., Mosley, J.R., Reilly, G.C., Reeve, J., Skerry, T.M., Lanyon, L.E., 2003. Mechanical loading: biphasic osteocyte survival and targeting of osteoclasts for bone destruction in rat cortical bone. The American Journal of Physiology-Cell Physiology. 284, C934-943. https://doi.org/10.1152/ajpcell.00234.2002

26. Oliveira, P.G.F.P. de, Bergamo, E.T.P., Neiva, R., Bonfante, E.A., Witek, L., Tovar, N., Coelho, P.G., 2018. Osseodensification outperforms conventional implant subtractive instrumentation: A study in sheep. Materials Science and Engineering C. Appl. 90, 300–307. https://doi.org/10.1016/j.msec.2018.04.051

27. Pai, U.Y., Rodrigues, S.J., Talreja, K.S., Mundathaje, M., 2018. Osseodensification - A novel approach in implant dentistry. The Journal of Indian Prosthodontics Society. 18, 196–200. https://doi.org/10.4103/jips.jips_292_17

28. Raggatt, L.J., Partridge, N.C., 2010. Cellular and Molecular Mechanisms of Bone Remodeling. The Journal of biological chemistry. 285, 25103–25108. https://doi.org/10.1074/jbc.R109.041087

29. Samsami, S., Saberi, S., Sadighi, S., Rouhi, G., 2015. Comparison of Three Fixation Methods for Femoral Neck Fracture in Young Adults: Experimental and Numerical Investigations. Journal of medical and biological engineering. 35, 566–579. https://doi.org/10.1007/s40846-015-0085-9

30. Sanders, E.R., 2012. Aseptic Laboratory Techniques: Volume Transfers with Serological Pipettes and Micropipettors. Journal of Visualized Experiments. JoVE. https://doi.org/10.3791/2754

31. Stocchero, M., Toia, M., Cecchinato, D., Becktor, J.P., Coelho, P.G., Jimbo, R., 2016. Biomechanical, Biologic, and Clinical Outcomes of Undersized Implant Surgical Preparation: A Systematic Review. The International Journal of Oral and Maxillofacial Implants. 31, 1247–1263.

32. Stokholm, R., Isidor, F., Nyengaard, J.R., 2014. Histologic and histomorphometric evaluation of peri-implant bone of immediate or delayed occlusal-loaded non-splinted implants in the posterior mandible--an experimental study in monkeys. Clinical Oral Implants Research. 25, 1311–1318. https://doi.org/10.1111/clr.12274

33. Suárez-González, D., Lee, J.S., Diggs, A., Lu, Y., Nemke, B., Markel, M., Hollister, S.J., Murphy, W.L., 2014. Controlled Multiple Growth Factor Delivery from Bone Tissue Engineering Scaffolds via Designed Affinity. Tissue Engineering Part A 20, 2077–2087. https://doi.org/10.1089/ten.tea.2013.0358

34. Summers, R.B., 1994. A new concept in maxillary implant surgery: the osteotome technique. Compendium. Newtown Pa 15, 152, 154–156, 158 passim; quiz 162.

35. Tretto, P.H.W., Fabris, V., Cericato, G.O., Sarkis-Onofre, R., Bacchi, A., 2018. Does the instrument used for the implant site preparation influence the bone-implant interface? A systematic review of clinical and animal studies. The International Journal of Oral and Maxillofacial Surgery. https://doi.org/10.1016/j.ijom.2018.04.005

36. Trisi, P., Berardini, M., Falco, A., Podaliri Vulpiani, M., 2016a. New Osseodensification Implant Site Preparation Method to Increase Bone Density in Low-Density Bone: In Vivo Evaluation in Sheep. Implant Dentistry. 25, 24–31. https://doi.org/10.1097/ID.0000000000000358

37. Trisi, P., Berardini, M., Falco, A., Podaliri Vulpiani, M., 2016b. New Osseodensification Implant Site Preparation Method to Increase Bone Density in Low-Density Bone: In Vivo Evaluation in Sheep. Implant Dentistry. 25, 24–31. https://doi.org/10.1097/ID.0000000000000358

38. Trisi, P., Perfetti, G., Baldoni, E., Berardi, D., Colagiovanni, M., Scogna, G., 2009. Implant micromotion is related to peak insertion torque and bone density. Clinical Oral Implants Research. 20, 467–471. https://doi.org/10.1111/j.1600-0501.2008.01679.x

39. Varnum-Finney, B., Xu, L., Brashem-Stein, C., Nourigat, C., Flowers, D., Bakkour, S., Pear, W.S., Bernstein, I.D., 2000. Pluripotent, cytokine-dependent, hematopoietic stem cells are immortalized by constitutive Notch1 signaling. Nature Medicine. 6, 1278–1281. https://doi.org/10.1038/81390

40. Vetsch, J.R., Müller, R., Hofmann, S., 2016. The influence of curvature on three-dimensional mineralized matrix formation under static and perfused conditions: an in vitro bioreactor model. Journal of the Royal Society, Interface. 13. https://doi.org/10.1098/rsif.2016.0425

CURRICULUM VITAE